Project Title: **Enhanced Power Stability for Proton Conducting Solid Oxides Fuel Cells**
Report Title: **Computational modeling, synthesis, and characterization of $BaZr_{1-x}Y_xO_{3-\delta}$ solid state proton conductor.**

Type of Report: Semi-Annual Technical Progress Report
Reporting Period Start Date: March 30, 2003
Reporting Period End Date: September 30, 2003

Principle Authors: Boris Merinov, Claudio O. Dorso, William A. Goddard III, Jian Wu, and Sossina Haile

Date Report was Issued: October 30, 2003

DOE Award Number: DE-FC26-02NT41631

Name and Address of Submitting Organization: California Institute of Technology, mail code 139-74, 1200 E. California Blvd., Pasadena, CA 91125

DISCLAIMER

ABSTRACT

During the second semiannual period we have carried out a series of QM calculations on the $BaZr_{1-x}Y_xH_xO_3$ proton conductor to determine the equilibrium proton positions and corresponding energies. We find that the size of the crystal cell is very important for the identification of the equilibrium proton positions. To derive ReaxFF parameters for Pt-surfaces and for H-transfer in Y-doped $BaZrO_3$, we carried out QM-calculations on the structures and energies of relevant condensed phases and cluster systems. These data then served as a training set to optimize the ReaxFF parameters. ReaxFF for various bulk metals (Pt, Zr, and Y) and metal clusters (Pt) was developed.

$BaZr_{1-x}Y_xO_{3-\delta}$ with x = 0.2, 0.3, 0.4, 0.5 was synthesized using a modified Pechini method and characterization (X-ray diffraction, scanning electron microscopy, and impedance spectroscopy) of this material was performed. We find that a *single perovskite phase* is formed in $BaZr_{1-x}Y_xO_{3-\delta}$.
The proton conductivity of $BaZr_{1-x}Y_xO_{3-\delta}$ with x = 0.5 is significantly lower than the conductivity of the samples with Y-dopant concentrations of 0.1 and 0.2.

TABLE OF CONTENTS

List of graphical materials ……. 5

Introduction …… 6

Executive summary …… 6

Results and discussion …… 7

Quantum Mechanical Calculations on $BaZr_{1-x}Y_xH_xO_3$ …….. 7

Development of ReaxFF to reproduce QM results …… 9

Synthesis of $BaZr_{1-x}Y_xO_{3-\delta}$ …… 11

Characterization of $BaZr_{1-x}Y_xO_{3-\delta}$…….…… 12

Conclusions ……... 14

References ……. 15

List of acronyms and abbreviations …….. 16

LIST OF GRAPHICAL MATERIALS

Fig.1. The best configurations for the different size systems of $BaZr_{0.5}Y_{0.5}H_{0.5}O_3$.

Fig.2. Polyhedral representation of the 2x2x2 crystal cell range of $BaZr_{0.5}Y_{0.5}H_{0.5}O_3$.

Fig.3. Relative energies for different configurations of $BaZr_{0.5}Y_{0.5}H_{0.5}O_3$.

Fig.4. Evolution of some parameters of the relaxation process for the best 2x2x2 configuration of $BaZr_{0.5}Y_{0.5}H_{0.5}O_3$.

Fig.5. QM- and ReaxFF results for the equation of state of various Zr-polymorphs.

Fig.6. QM- and ReaxFF results for the equations of state of various Pt-polymorphs.

Fig.7. QM- and ReaxFF results for the equations of state of various Y-polymorphs.

Fig.8. Relative energies for Pt-clusters from QM- and ReaxFF.

Fig.9. X-ray diffraction patterns of $BaZr_{1-x}Y_xO_{3-\delta}$ powders calcined at 1250°C for 10 hours.

Fig.10. Plot of the refinement of the $BaZr_{1-x}Y_xO_{3-\delta}$ lattice parameters.

Fig.11. SEM image of $BaZr_{0.5}Y_{0.5}O_{2.75}$.

Fig.12. Temperature dependence of the proton conductivity of $BaZr_{0.5}Y_{0.5}O_{2.75}$.

INTRODUCTION

Many acceptor-doped perovskite-type oxides show high protonic conductivity at elevated temperatures. Akaline-earth cerates and zirconates such as $BaCeO_3$ and $BaZrO_3$ are among of them. In addition to their reduced temperature operation relative to traditional oxide ion conductors such as Y-stabilized ZrO_2, these perovskites, because of their proton transport properties, offer the possibility of application in a number of arenas including hydrogen sensors for molten metals, H_2/D_2 separators, and hydrogen pumps. However, doped $BaCeO_3$ shows quite poor mechanical and chemical stability that make its application in fuel cell problematic. In this situation, Y-doped $BaZrO_3$ is becoming one of the most promising proton conducting materials for SOFC applications. It has desirable properties such as high protonic conductivity and excellent chemical and mechanical stability. The current limitation for application of Y-doped $BaZrO_3$ in PC SOFCs is the extremely high grain boundary resistance, which leads to the relatively poor total conductivity. To understand the conduction process (both bulk and grain boundary) as well as the role of defects and dopants in transport at the molecular level, we are developing the multi-scale strategy based on accurate QM calculations of the relevant materials which are then used to derive a First Principles-based ReaxFF allowing large-scale MD simulations that enable the study of proton transport under realistic conditions (temperature, structure, etc.) as well as the role of grain boundaries, defects, etc. Follow-up experiments are used to validate the computational predictions as well as to formulate new problems and tasks.

EXECUTIVE SUMMARY

A series of QM calculations on the $BaZr_{1-x}Y_xH_xO_3$ proton conductor have been performed to determine the equilibrium proton positions and corresponding energies. The system, on which we mostly focused, was $BaZr_{0.5}Y_{0.5}H_{0.5}O_3$. It was shown that the size of the crystal cell range is very important for the identification of the equilibrium proton positions. The calculations in larger crystal cell ranges provide a remarkably better set of configurations.

To develop ReaxFF parameters for electrode surfaces and for proton transfer in the Y-doped $BaZrO_3$ solid electrolyte, we are currently performing QM-calculations on the structures and energies of relevant condensed phases and cluster systems. These data serve as a training set to compare and optimize the ReaxFF parameters. At present, we have the ReaxFF description for various bulk metals (Pt, Zr, and Y) and metal clusters (Pt).

A modified Pechini route was successfully used for synthesis a single perovskite phase of the proton conducting $BaZr_{1-x}Y_xO_{3-\delta}$ solid oxides with wide range of the Y dopant concentration. X-ray diffraction, scanning electron microscopy, and impedance spectroscopy were performed on $BaZr_{0.5}Y_{0.5}O_{2.75}$. The proton conductivity was measured over the extended temperature range and at different atmospheres. It turned out that the conductivity of $BaZr_{0.5}Y_{0.5}O_{2.75}$ is significantly lower than, for instance, that of the samples with Y-dopant concentrations of 0.1 and 0.2. It seems that the high concentration of the Y-dopant might lead to a trapping of the protons.

RESULTS AND DISCUSSION

THEORETICAL

In order for theory to make fundamental contributions to the design and optimization of a fuel cell it must be based on First Principles, using experimental data only for validation purposes. Thus, we use *ab initio* QM to investigate mechanisms of chemical reactions and proton migration. However, applications of QM methods are limited to small model systems and short time scales. To predict important performance characteristics of fuel cell devices, we develop ReaxFF based on the *ab initio* QM methods but practical for MD and KMC simulations of systems containing thousands and millions of atoms for relatively long times (~100 nanoseconds). Our recent advance in developing ReaxFF [1,2] should extend the accuracy of QM to provide an adequate description of the fundamental reaction mechanisms that control the efficiency of PC SOFC.

Quantum Mechanical Calculations on $BaZr_{1-x}Y_xH_xO_3$

Our current quantum mechanical (QM) calculations are based on Density Functional Theory (DFT) [3,4] using Generalized Gradient Approximation (GGA) [5] to treat the exchange-correlation energy functional [6]. In these calculations pseudopotentials are used to replace the core electrons. All calculations are performed at T = 0K. The calculations use 3D periodic boundary conditions. The QM calculations are carried out using the pseudo-potential local basis set code SeqQuest, jointly being developed between Sandia National Laboratories (Dr. Peter Schultz) and Caltech.

During the second semiannual period we have performed a series of QM calculations on the $BaZr_{1-x}Y_xH_xO_3$ proton conductor to determine the equilibrium proton positions and corresponding energies. We have focused on the system with the 50% concentration of Y ($BaZr_{0.5}Y_{0.5}H_{0.5}O_3$). This concentration has been chosen because

- according to the simple percolation arguments it might lead to higher proton conductivity in homogeneous systems,
- it could be analyzed with a smaller number of unit cells (2x1x1) that allows faster screening various conformations.

After extensive convergence tests we had found optimal parameters (such as number of k-points, grids for numerical integrations, etc.) for the following *ab initio* calculations which were focused on

- characterization of the local structures around the Y and H defects,.
- determination of the structure-energy relationships,
- exploring the effect of the system size on the structures and energetics.

Fig.1 shows the best configurations obtained from our analysis of the different size systems. The importance of the octahedral orientations could be seen in Fig.2. In order to see and analyze how the tilt of the octahedra influences on the relaxation process, the size of the crystal cell range should be at least 2x2x2.

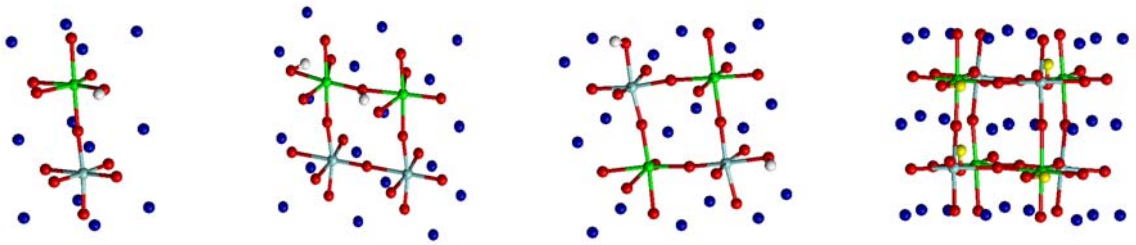

a *b* *c* *d*

Fig.1. The best configurations for the different size systems of $BaZr_{0.5}Y_{0.5}H_{0.5}O_3$.
Y-green, Zr – light blue, Ba – blue, O – red, and H – white.
a - the 2x1x1 crystal cell range, *b* - the 2x2x1 crystal cell range, *c* - the 2x2x1 crystal cell range,
d - the 2x2x2 crystal cell range.

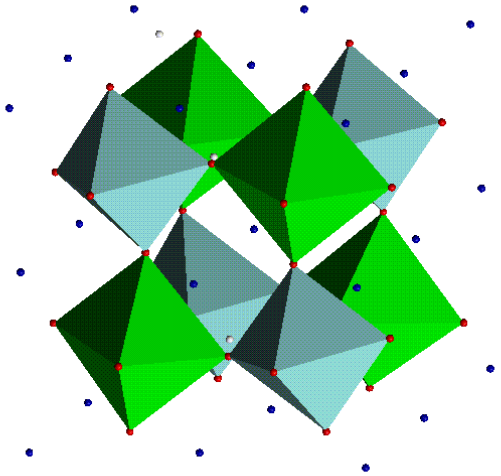

Fig.2. Polyhedral representation of the 2x2x2 crystal cell range of $BaZr_{0.5}Y_{0.5}H_{0.5}O_3$.

Fig.3 shows energy differences related to the overall best configuration. It is clearly seen that the size of the crystal cell range is very important for the identification of the equilibrium proton positions. The calculations in larger crystal cell ranges provide a remarkably better set of configurations than more simple sets denoted in the Fig.3 as b) and c).

We are currently working on deriving a simple model description of the *ab initio* energetics in terms of the variation of the bond order of the Y and Zr atoms caused by the protons which make the metal-O bonds weaker. Such a description might be extremely valuable for mesoscopic simulations of proton conduction in ceramics.

Finally, Fig.4 shows the evolution of the total energy, electrostatic energy, and three diagonal components of the stress tensor as a function of the relaxation process steps for the best 2x2x2 configuration. Fig.4d shows steps at which changes of the cell volume occurs (each horizontal segment corresponds to some constant value of the volume).

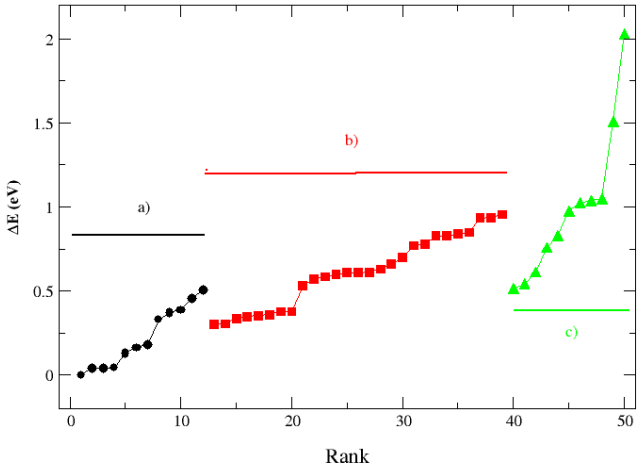

Fig.3. Relative energies for different configurations of $BaZr_{0.5}Y_{0.5}H_{0.5}O_3$.
Black circles: a set of configurations for the 2x2x2 crystal cell range, red squares: a set of the *b* configurations (see Fig.2) for the 2x2x1 crystal cell range, green triangles: a set of the *c* configurations (see Fig.2) for the 2x2x1 crystal cell range.

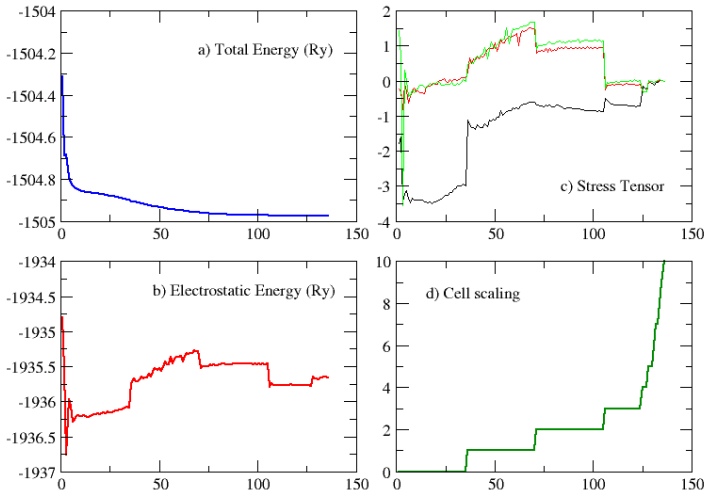

Fig.4. Evolution of some parameters of the relaxation process for the best 2x2x2 configuration of $BaZr_{0.5}Y_{0.5}H_{0.5}O_3$.

Development of ReaxFF to reproduce QM results

In order to simulate the reactions in PC SOFC we are now developing ReaxFF for a number of different systems. Our current ReaxFF development is focusing on two aspects of fuel cell chemistry:

(1) H-transfer in Y-doped $BaZrO_3$ fuel cell-electrolyte and
(2) catalytic reactions at Pt-electrode surfaces.

ReaxFF should allow us to perform detailed atomistic simulations of reactive processes pertinent to fuel cell chemistry on system sizes (>1000 atoms) that are too large to be amenable to QM methods, but which will give back accuracy for barriers and process comparable to QM.

To derive ReaxFF parameters for Pt-surfaces and for H-transfer in Y-doped $BaZrO_3$, we first carried out QM-calculations on the structures and energies of relevant condensed phases and cluster systems. These data then serve as a training set to compare and optimize the ReaxFF parameters. We currently have the ReaxFF description for various bulk metals (Pt, Zr, and Y) and metal clusters (Pt).

Bulk metals. For each of the metal atoms in a Pt/Y-doped $BaZrO_3$-fuel cell we carried out QM-simulations to determine EOS of several polymorphs. These data are subsequently used to derive ReaxFF parameters.

Figs.5-7 compare the QM-data to the ReaxFF results. Most weight was given in the ReaxFF parameter optimization to the low-energy phases. For the high-energy phases (i.e. simple cubic (sc) and diamond), we gave little weight to the QM-equation of state but rather focused on making sure that ReaxFF gets the correct energy with respect to the low-energy phases.

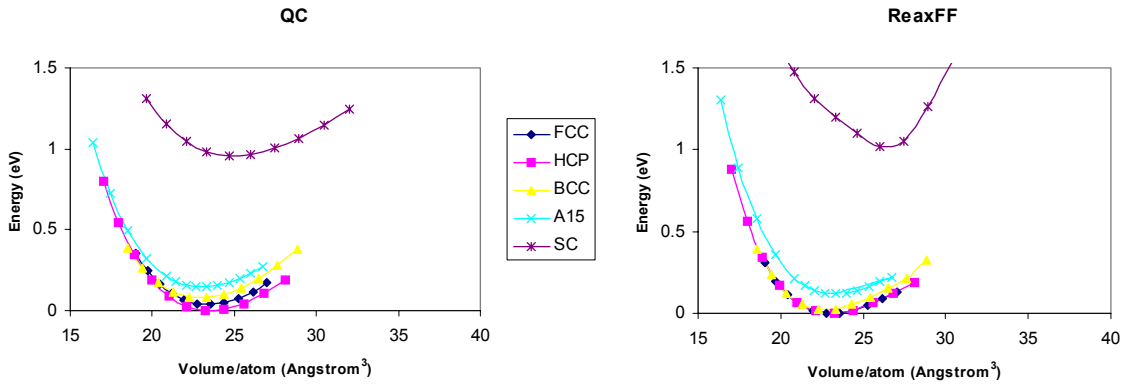

Fig5. QM- and ReaxFF results for the equation of state of various Zr-polymorphs.

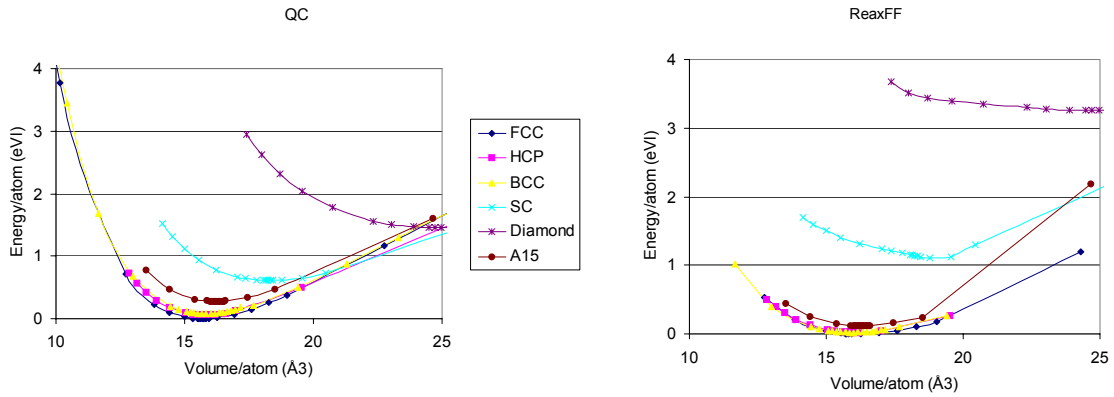

Fig.6. QM- and ReaxFF results for the equations of state of various Pt-polymorphs.

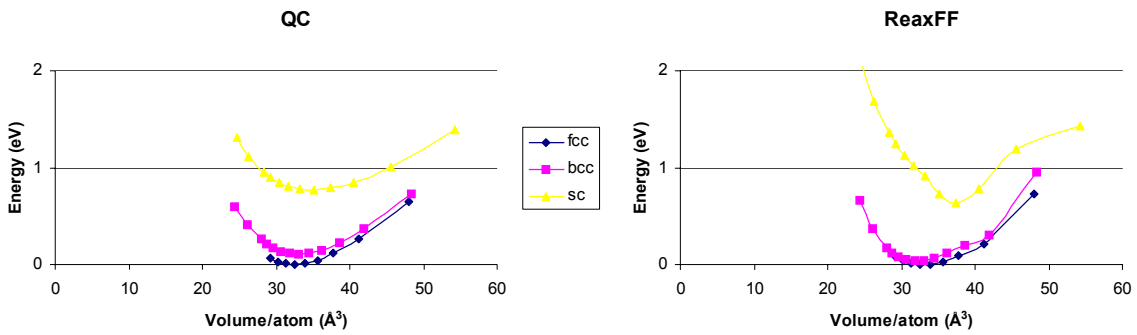

Fig.7. QM- and ReaxFF results for the equations of state of various Y-polymorphs.

For each metal we fitted the ReaxFF parameters against the cohesive energy for the most stable bulk phase. Table 1 compares the ReaxFF results to literature values.

Table 1. Cohesive energies for bulk metal phases (in eV) for ReaxFF compared to experiment (Handbook of Chemistry and Physics, 81st edition).

Metal	ReaxFF	Literature
Pt	6.05	6.31
Zr	5.99	6.25
Y	3.87	4.37

Metal clusters. As the Pt in the anode and cathode are likely to be highly dispersed Pt, with particle sizes of ~ 2 nm diameter, we also fitted the Pt-ReaxFF parameters against the cohesive energy for various clusters of Pt atoms. Fig.8 compares the stabilities for these clusters from ReaxFF and QM.

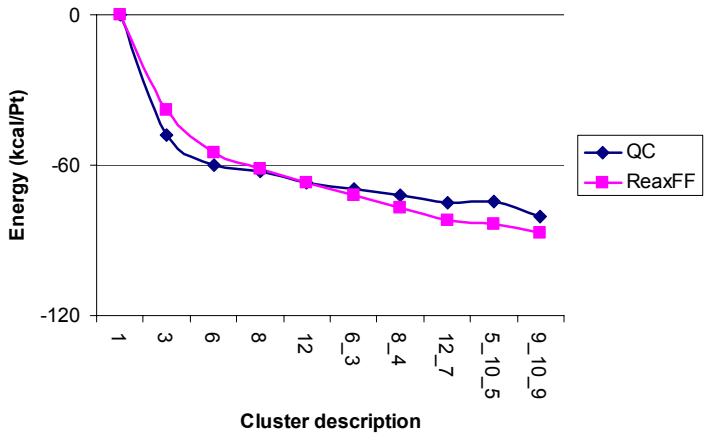

Fig.8. Relative energies for Pt-clusters from QM- and ReaxFF.
All clusters were fixed in the fcc-configuration; the cluster notation describes the number of layers and the number of atoms in each layer. For example, 12_7 is a 2-layer cluster with 12 atoms in the first and 7 atoms in the second layer.

EXPERIMENTAL

Synthesis of $BaZr_{1-x}Y_xO_{3-\delta}$

$BaZr_{1-x}Y_xO_{3-\delta}$ with x = 0.2, 0.3, 0.4, 0.5 was synthesized by a modified Pechini route [7]. The precursors were $Ba(NO_3)_2$, $Y(NO_3)_3{\cdot}6H_2O$ and $ZrO(NO_3)_2{\cdot}xH_2O$ (x was determined by thermo-gravimetric analysis to be 1.96). EDTA and EG were used as polymerization/complexation agents at molar ratios of EDTA/ΣMetal = 2.0 and EDTA/EG=1/3. The powders derived were calcined at 1250°C for 10 hours.

XRD patterns of the samples were collected by a Philips X'pert Pro diffractometer using CuKα radiation. Fig.9 shows the XRD patterns of the powders calcined at 1250°C for 10 hours.

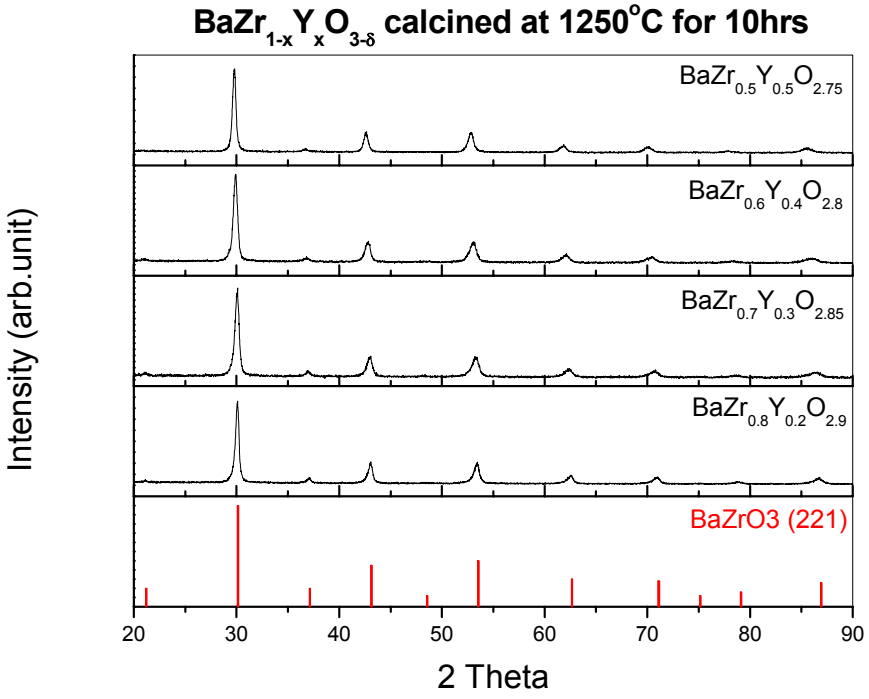

Fig.9. X-ray diffraction patterns of $BaZr_{1-x}Y_xO_{3-\delta}$ powders calcined at 1250°C for 10 hours.

The XRD patterns indicate that a single perovskite phase is formed in $BaZr_{1-x}Y_xO_{3-\delta}$ (x = 0.2-0.5). The peaks shift to the lower 2θ with increasing x, which could be explained by the ion size difference between Y^{3+}(0.892Å) and Zr^{4+}(0.72 Å). Therefore, the modified Pechini method can successfully be used for the synthesis of the proton conducting $BaZr_{1-x}Y_xO_{3-\delta}$ solid oxides with a wide range of the dopant concentration.

Since the computational study was mostly focused on $BaZr_{0.5}Y_{0.5}H_{0.5}O_3$, our experimental work in this semiannual period was also focused on this material.

Characterization of $BaZr_{1-x}Y_xO_{3-\delta}$

The plot of the refinement of the $BaZr_{1-x}Y_xO_{3-\delta}$ lattice parameters is shown in Fig.10. The X'plus program was used to refine the cubic lattice parameters. It is clearly seen that the lattice parameters grow up with increasing x and at x = 0.5 ($BaZr_{0.5}Y_{0.5}O_{2.75}$) they reach the value of 4.2487(4) Å, cubic symmetry, space group Pm-3m.

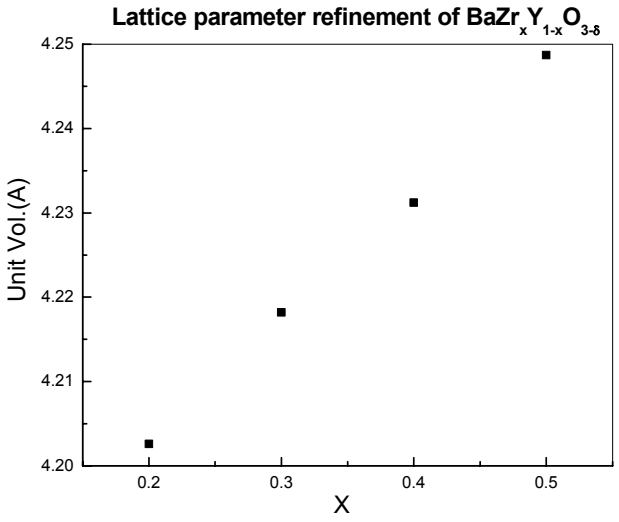

Fig.10. Plot of the refinement of the $BaZr_{1-x}Y_xO_{3-\delta}$ lattice parameters.

Fig.11 shows the SEM image of $BaZr_{0.5}Y_{0.5}O_{2.75}$ sintered at 1550°C/8h, relative density = 4.775/5.96 = 80%. The sample consists of fine and homogeneous grains, ~200 nm, similar to most of the unmodified $BaZrO_3$.

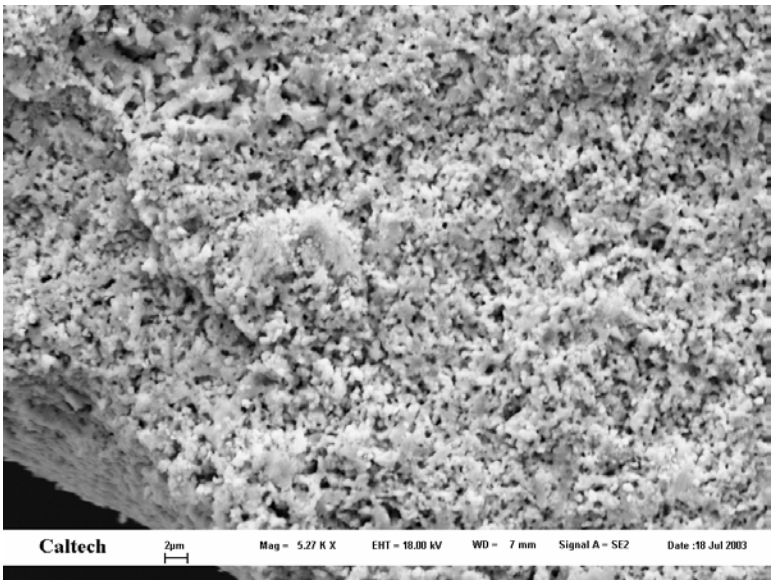

Fig.11. SEM image of $BaZr_{0.5}Y_{0.5}O_{2.75}$.

The transport property of $BaZr_{0.5}Y_{0.5}O_{2.75}$ can be seen in Fig.12. The proton conductivity data were obtained from impedance spectroscopy on $BaZr_{0.5}Y_{0.5}O_{2.75}$ over the extended temperature

range and at different atmospheres. It turned out that the conductivity of $BaZr_{0.5}Y_{0.5}O_{2.75}$ is significantly lower than, for instance, that of $BaZr_{0.9}Y_{0.1}O_{2.95}$ [8]. It seems that the high concentration of the Y-dopant might lead to a trapping of the protons.

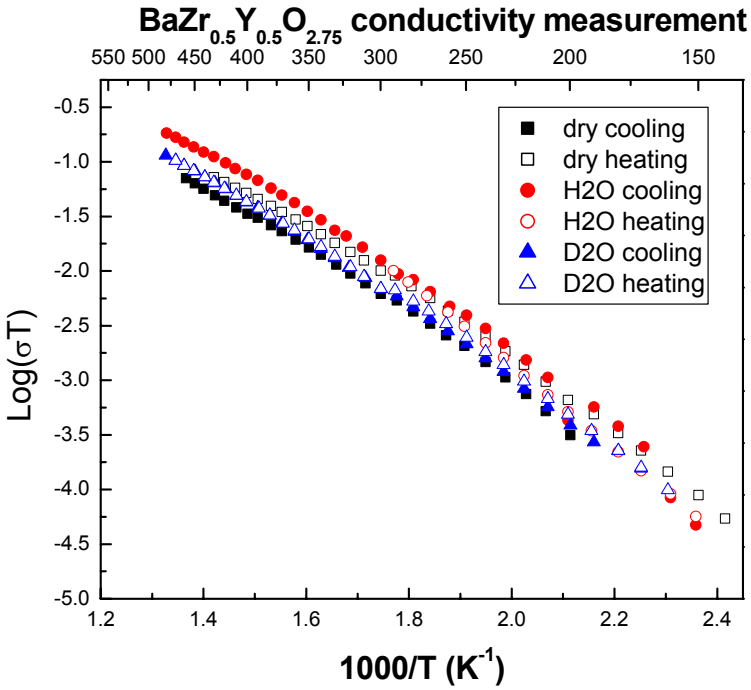

Fig.12. Temperature dependence of the proton conductivity of $BaZr_{0.5}Y_{0.5}O_{2.75}$.

CONCLUSIONS

We carried out a series of QM calculations on $BaZr_{0.5}Y_{0.5}H_{0.5}O_3$ to determine the equilibrium proton positions and corresponding energies. We find that the larger crystal cell range used in the calculations provide the energetically better set of configurations.

To derive ReaxFF parameters for Pt-surfaces and for H-transfer in Y-doped $BaZrO_3$, we carried out QM-calculations on relevant condensed phases and cluster systems.

We developed ReaxFF for various bulk metals (Pt, Zr, and Y) and metal clusters (Pt).

We synthesized $BaZr_{1-x}Y_xO_{3-\delta}$ with x = 0.2, 0.3, 0.4, 0.5 using a modified Pechini method. We find that a single perovskite phase is formed in $BaZr_{1-x}Y_xO_{3-\delta}$.

Characterization (X-ray diffraction, scanning electron microscopy, and impedance spectroscopy) of $BaZr_{1-x}Y_xO_{3-\delta}$ has been performed. Proton conductivity of $BaZr_{1-x}Y_xO_{3-\delta}$ with x = 0.5 is significantly lower than the conductivity of the samples with Y-dopant concentrations of 0.1 and 0.2.

In the forthcoming months we will perform the following calculations:

We will continue exploring the energy landscape for the equilibrium proton positions in $BaZr_{1-x}Y_xO_{3-\delta}$ with various dopant concentrations.

We will continue developing ReaxFF, which will be applied for MD simulations of different processes in the $BaZr_{1-x}Y_xO_{3-\delta}$ solid electrolyte and electrode/electrolyte interface area. For this, further QM-calculations on the structures and energies of relevant condensed phases and cluster systems will be performed.

Structural and chemical stability of $BaZr_{1-x}Y_xO_{3-\delta}$ with various dopant concentrations will be studied by both calculation and experimental route.

Sintering and transport properties of $BaZr_{1-x}Y_xO_{3-\delta}$ will be investigated experimentally.

REFERENCES

1. A. C. T. van Duin, S. Dasgupta, F. Lorant, and W. A. Goddard, *J. Phys. Chem.* **A105** 9396 (2001).
2. A. C. T. van Duin, A. Strachan, S. Stewman, Q. Zhang, X. Xu, and W. A. Goddard, *J. Phys. Chem.* **A107** 3803 (2003).
3. P.Hohenberg and W.Kohn*, Phys. Rev*. **136** 864B (1964).
4. W.Kohn and L. J. Sham, *Phys. Rev*. **140** 1133A (1965).
5. J. P. Perdew, K.Burke and M. Ernzerhof, *Phys. Rev. Lett. 77* 3865 (1996).
6. W.G.Hoover *Phys. Rev. A***31** 1695 (1985).
7. V.Agarwal and M. Liu, *J. Mat. Sci.* **32** 619 (1997).
8. H.G. Bohn and T. Schober, *J. Am. Ceram. Soc.* **83** 768 (2000).

LIST OF ACRONYMS AND ABBREVIATIONS

DFT - Density Functional Theory,

EDTA – Ethylene Diamine Tetraacetic Acid

EG – Ethylene Glycol

EOS - Equation of States,

GGA - Generalized Gradient Approximation,

KMC - Kinetic Monte Carlo,

MD - Molecular Dynamics,

NVT – Constant-volume/Constant-temperature dynamics.

PC SOFC – Proton Conducting Solid Oxide Fuel Cell,

QM - Quantum Mechanics,

ReaxFF - First Principles-Based Reactive Force Field,

SEM – Scanning Electron Microscopy

XRD – X-ray Diffraction